Mon. Not. R. Astron. Soc. **000**, 000–000 (0000) Printed 2 October 2014 (MN LATEX style file v2.2)

On the observability of coupled dark energy with cosmic voids

P. M. Sutter[1,2,3] ⋆, Edoardo Carlesi[4], Benjamin D. Wandelt[1,2,5,6], and Alexander Knebe[4]

[1] *Sorbonne Universités, UPMC Univ Paris 06, UMR7095, Institut d'Astrophysique de Paris, F-75014, Paris, France*
[2] *CNRS, UMR7095, Institut d'Astrophysique de Paris, F-75014, Paris, France*
[3] *Center for Cosmology and Astro-Particle Physics, Ohio State University, Columbus, OH 43210*
[4] *Departamento de Física Teórica, Universidad Autónoma de Madrid, 28049, Cantoblanco, Madrid, Spain*
[5] *Department of Physics, University of Illinois at Urbana-Champaign, Urbana, IL 61801*
[6] *Department of Astronomy, University of Illinois at Urbana-Champaign, Urbana, IL 61801*

arXiv:1406.0511v2 [astro-ph.CO] 1 Oct 2014

2 October 2014

ABSTRACT

Taking N-body simulations with volumes and particle densities tuned to match the SDSS DR7 spectroscopic main sample, we assess the ability of current void catalogs (e.g., Sutter et al. 2012b) to distinguish a model of coupled dark matter-dark energy from ΛCDM cosmology using properties of cosmic voids. Identifying voids with the `VIDE` toolkit, we find no statistically significant differences in the ellipticities, but find that coupling produces a population of significantly larger voids, possibly explaining the recent result of Tavasoli et al. (2013). In addition, we use the universal density profile of Hamaus et al. (2014) to quantify the relationship between coupling and density profile shape, finding that the coupling produces broader, shallower, undercompensated profiles for large voids by thinning the walls between adjacent medium-scale voids. We find that these differences are potentially measurable with existing void catalogs once effects from survey geometries and peculiar velocities are taken into account.

Key words: cosmology: simulations, cosmology: large-scale structure of universe

1 INTRODUCTION

Even though a variety of cosmological tests demonstrate that the inflation plus cold dark matter (ΛCDM) paradigm is extremely successful in describing the history and structure of the Universe (e.g., Reid et al. 2012; Planck Collaboration 2013), there are still several features of the large-scale distribution of matter that are difficult to explain. One is the so-called "void phenomenon", first noticed by Peebles (2001), in which cosmic voids — the deep underdensities in the galaxy distribution — appear emptier than expected from N-body simulations.

The observation of this phenomenon motivated the development of models in which a dynamical scalar field responsible for dark energy (DE; Peebles & Ratra 1988; Ratra & Peebles 1988) is coupled to the dark matter (DM), giving an additional fifth force of nature that would help empty out the voids (Nusser et al. 2005). Other possibilities to explain the void phenomenon have since been proposed, including modified gravity (e.g., Li & Zhao 2009; Clampitt et al. 2013; Spolyar et al. 2013) and an improved understanding of the relationship between galaxy formation and environment (Tinker & Conroy 2009; Kreckel et al. 2011).

Most analyses of coupled DM-DE have focused on the statistics of overdense regions, such as the halo mass function (Sutter & Ricker 2008), the galaxy two-point correlation function (Carlesi et al. 2014) and galaxy cluster gas properties (Baldi et al. 2010; Carlesi et al. 2014). However, in these high-density environments it is difficult to distinguish effects due to coupling from non-linear evolution and complex baryonic physics.

Focusing on underdense regions would appear to be a more natural way to study the void phenomenon. On the theory side, studies have considered the effect of coupling in the dark sector on the void number function (Clampitt et al. 2013), density profiles (Spolyar et al. 2013), and shapes (Li & Zhao 2009; Li et al. 2012). Observationally, void populations in galaxy surveys can be compared to expectations from simulations (e.g., Muller et al. 2000; Pan et al. 2012). Most recently, the study of Sutter et al. (2013) found no evidence for departures from ΛCDM for a population of voids at higher redshift ($z \sim 0.4 - 0.7$), but Tavasoli et al. (2013)

⋆ Email: sutter@iap.fr

© 0000 RAS

noted the existence of a large void that appears to be statistically incompatible with predictions of ΛCDM N-body simulations.

This comparative inattention to voids themselves can be explained by the relative dearth of voids in observations and the lack of robust void statistical tools that can be used to connect theoretical results to observational reality. However, there have been significant advancements in the past few years, including the release of large public void catalogs (Pan et al. 2012; Sutter et al. 2012b, 2013) from the SDSS galaxy surveys (Abazajian et al. 2009; Ahn et al. 2012). Secondly, there has been significant efforts to single out especially sensitive void properties and make predictions for the void signals in data (e.g., Lavaux & Wandelt 2010; Biswas et al. 2010; Bos et al. 2012; Jennings et al. 2013; Sutter et al. 2013) The combination of enhanced tools and a statistically meaningful sample of voids means that predictions of the effects of coupled DM-DE within voids can now make direct contact with data.

In this *letter* we provide an initial assessment of the impact of coupled DM-DE on void statistics such as number functions, ellipticities, and radial density profiles. While this work is similar to that of Li (2011), we particularly focus on the ability of current low-redshift galaxy surveys such as the SDSS DR7 (Ahn et al. 2012) to distinguish coupled models from ΛCDM with the population of voids identified in their limited volumes and galaxy densities (Pan et al. 2012; Sutter et al. 2012b). We also incorporate the latest theoretical work, such as the recently-described universal density profile (Hamaus et al. 2014; hereafter HSW), to understand and quantify our results.

In the following section we briefly present the quintessence model, its implementation in simulation, and our method for finding voids. In Section 3 we discuss the effects on void properties, and conclude in Section 4 with comments on the relevancy for current surveys and outline strategies for more complete analyses in the future.

2 SIMULATIONS & VOID FINDING

Under quintessence the dark energy scalar field ϕ has the Lagrangian

$$L = \int d^4x\sqrt{-g}\left(-\frac{1}{2}\partial_\mu\partial^\mu\phi + V(\phi) + m(\phi)\psi_m\bar{\psi}_m\right), \quad (1)$$

where ϕ interacts with the matter field ψ_m through the mass term of the dark matter particles. In this work we assume the Ratra & Peebles (1988) self interaction potential:

$$V(\phi) = V_0\left(\frac{\phi}{M_p}\right)^{-\alpha} \quad (2)$$

where M_p is the Planck mass and V_0 and α are two parameters that must be fixed by fitting to observations (Wang et al. 2012; Chiba et al. 2013).

Under this interaction the dark matter particle mass evolves as

$$m(\phi) = m_0\exp\left(-\beta(\phi)\frac{\phi}{M_p}\right). \quad (3)$$

This evolution implies that the dark matter particles experience an effective gravitational constant of the form (Baldi et al. 2010):

$$\tilde{G} = G_N(1 + 2\beta^2(\phi)) \quad (4)$$

where G_N is the standard Newtonian value. We will fix the interaction term to be constant such that $\beta(\phi) = \beta$. This leads to a dark matter particle mass that decreases as a function of time to its $z = 0$ ΛCDM value. For this work, we contrast a ΛCDM case with a single interacting model with parameters $V_0 = 10^{-7}$, $\alpha = 0.143$, and $\beta = 0.099$ (hereafter referred to as cDE).

We used the simulations described in Carlesi et al. (2014) and Carlesi et al. (2014) for this analysis. Briefly, these interactions were implemented with a modified version of the Tree-PM code `GADGET-2` (Springel 2005), with initial conditions generated using a version of the `N-GenIC` code suitably modified to account for the interactions. Both simulations had identical initial random phases, and were generated using a first order Zel'dovich approximation with suitable modifications to account for cDE. The cosmological parameters used in both ΛCDM and cDE simulations were $h = 0.7$, $n = 0.951$, $\Omega_{dm} = 0.224$, $\Omega_b = 0.046$, and $\sigma_8 = 0.8$ (normalized at $z = 0$) and were constructed to have dark matter power spectra within current observational limits.

These simulations took place in a cubic volume of 250 h^{-1}Mpc per side using 1024^3 DM amd 1024^3 gas particles. We ignored the gas particles and randomly subsampled the $z = 0.1$ dark matter particles to achieve a mean density of $\bar{n} = 4 \times 10^{-3}$ per cubic h^{-1}Mpc. This combination of simulation volume, density, and redshift approximates the *dim2* volume-limited SDSS galaxy sample used in Sutter et al. (2012b). We subsample the simulations to have identical numbers of particles. While DM-DE coupling would presumably change the luminosity function of galaxies, leading to a change in the total number of galaxies in a magnitude-limited survey, we are modeling a *volume*-limited survey, which will have identical number counts in each scenario (assuming that the change in galaxy abundances occurs below the magnitude threshold of the survey). Additionally, Sutter et al. (2013) found that bias does not greatly impact ($< 10\%$) void density profiles and abundances, and that the effects of bias are constant across difference cosmological models. In summary, to examine the impact of DM-DE coupling in a realistic scenario we may ignore galaxy (and halo) bias and work only with subsampled dark matter.

We identify voids with the `VIDE` toolkit (Sutter et al. 2014), which uses `ZOBOV` (Neyrinck 2008) to construct a Voronoi tessellation of the tracer particles and apply the watershed transform to group basins into voids. As in Sutter et al. (2012b), we remove voids smaller than the mean particle separation (6.3 h^{-1}Mpc) and those with central densities higher than 0.2 the mean particle density $\bar{n}$. Additionally, to limit the growth of voids we set a threshold of $0.2\bar{n}$ for joining additional zones into voids (see Neyrinck (2008) for a discussion). If a void consists of only a single zone then this restriction does not apply.

3 RESULTS

Figure 1 shows the cumulative number function for the ΛCDM and cDE simulations. We immediately note the presence of large voids in the cDE simulation, well beyond the

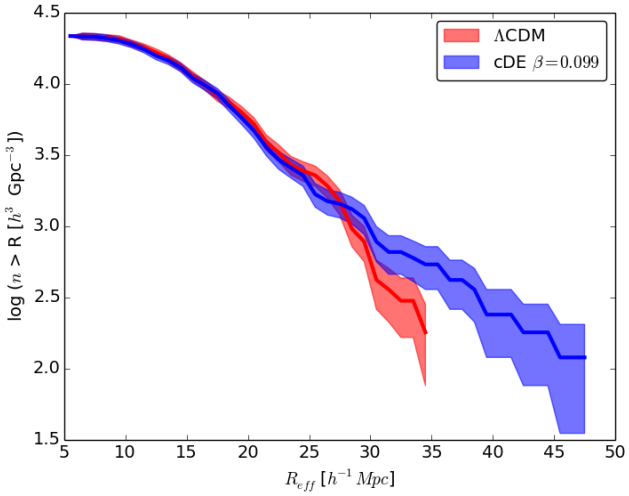

Figure 1. Cumulative void number functions. Shown are abundances for ΛCDM (red) and cDE (blue) models from subsampled N-body simulations. The solid lines are the measured number functions and the shaded regions are the 1σ Poisson uncertainties. For the same σ_8, cDE results in an excess of large scale voids and a deficit of medium scale voids compared to ΛCDM.

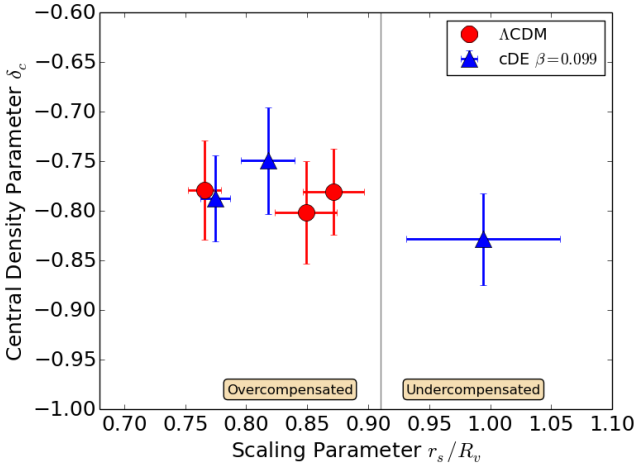

Figure 4. Best-fit values and 1σ uncertainties for all void stacks studied using the profile given by Eq. (5). Shown are values from ΛCDM (red circles) and cDE (blue triangles). The thin grey line depicts compensation scale. For each sample from left to right the points are for the $10-20$, $20-30$, and $30-40$ h^{-1}Mpc stacks.

largest voids in the ΛCDM simulation. However, for smaller void sizes ($R_{\rm eff} < 20$ h^{-1}Mpc) the two void populations are almost indistinguishable. The total number of voids in both models is nearly the same due to our fixing of $\sigma_8 = 0.8$, since constraining the freedom of this parameter implies that at least some statistical properties of the cosmic web must be retained when departing from ΛCDM. Also, the model we consider here has only modest ($< 2\%$) departures from standard gravity.

To interpret these results we match voids in ΛCDM to voids in the cDE simulation using the approach described in Sutter et al. (2014): a "match" is a corresponding void whose center lies within the void under consideration and has the most amount of shared particles. The former condition prevents matching to voids in the nearby volume that only happen to share a few edge particles. Figure 2 shows the relative radius ($R_{\rm eff,cDE}/R_{\rm eff,\Lambda CDM}$) and relative macrocenter distance ($d/R_{\rm eff,\Lambda CDM}$) for the matched voids. With this insight we see that while the largest voids are largely unaffected, small- and medium-scale voids generally experience radii inflation of $10-20\%$, and occasionally dramatic increases of up to a factor of two. The right panel of Figure 2 reveals why: larger relative radii tend to correspond to large relative distances, up to the ΛCDM void effective radius. Thus the walls between medium-scale voids are thinned out enough in the presence of cDE to allow the watershed to merge them together into a single larger void. This explains the feature at ~ 25 h^{-1}Mpc in the cDE number function: these ΛCDM voids are merging together to form the largest cDE voids. The primary cause of this thinning out, whether the modified expansion history or the fifth force itself, requires more investigation.

In Figure 3 we show one-dimensional radial profiles for all samples in radius bins of width 10 h^{-1}Mpc. To compute the profiles we take all voids in the radius bin, align all their macrocenters, and measure the total density in thin spherical shells. We normalize each density profile to the mean number density of the sample and show all profiles as a function of the relative radius, R/R_v, where R_v is the median void size in the stack. We do not individually rescale the voids since that tends to dampen the compensation region (Sutter et al. 2012a), which we wish to highlight in this analysis.

The profiles in each stack follow the same overall structure (a deeply-underdense core, a steep wall, an overdense "compensation" shell, and a flattening to the mean density); however, there are some contrasts between ΛCDM and cDE voids. First, while there are almost no differences between ΛCDM and cDE voids at the smallest scales, greater discrepancies appear for the larger (> 20 h^{-1}Mpc) stacks. From 20 to 30 h^{-1}Mpc, cDE voids have higher compensation shells, but after 30 h^{-1}Mpc the cDE voids are clearly larger and flatter (i.e., lower density contrast between wall and center). This difference in the largest stack is statistically highly significant.

To quantify and understand these differences, we fit all the profiles to the universal function presented in HSW:

$$\frac{n}{\bar{n}}(r) = \delta_c \frac{1-(r/r_s)^{\alpha(r_s)}}{1+(r/R_v)^{\beta(r_s)}} + 1, \quad (5)$$

While there are four parameters total in the model, HSW describe a two-parameter reduced model where

$$\alpha(r_s) \simeq -2.0(r_s/R_v) + 4.0 \quad (6)$$

$$\beta(r_s) \simeq \begin{cases} 17.5(r_s/R_v) - 6.5 & \text{if } r_s/R_v < 0.91 \\ -9.8(r_s/R_v) + 18.4 & \text{if } r_s/R_v > 0.91. \end{cases} \quad (7)$$

This two-parameter model describes all but the largest voids very accurately, and is appropriate for the analysis here (Sutter et al. 2013). There are two free parameters to this model: r_s, the radius at which the profile reaches mean density, and δ_c, the density in the central core. Figure 4 shows all best-fit values of δ_c and r_s for all stacks in both simulations.

The fitting parameters elucidate the relationship between DM-DE coupling and profile shape. All voids in all models maintain roughly the same central density of

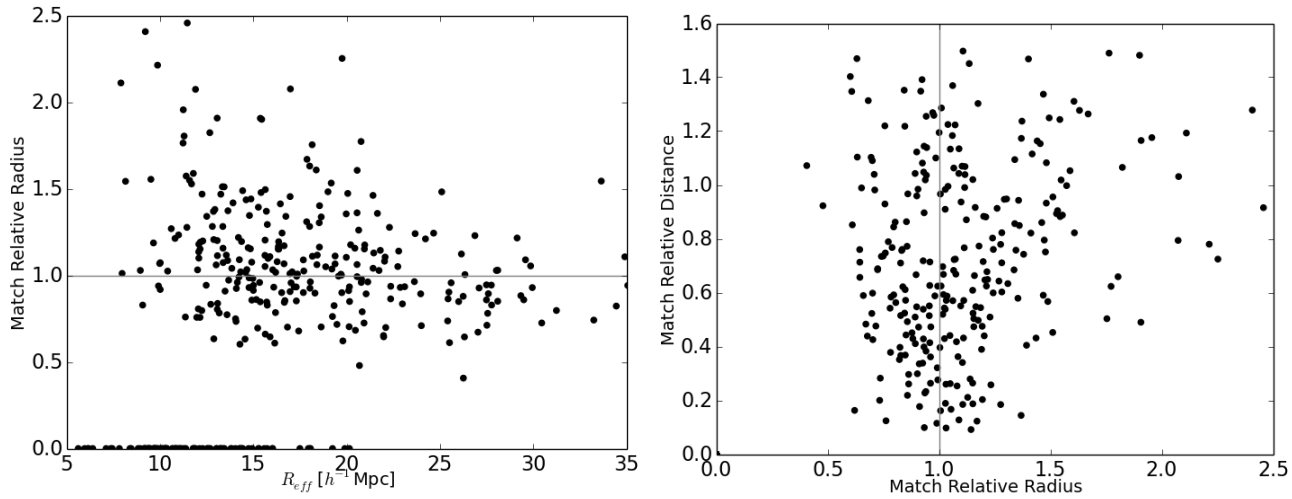

Figure 2. Relative properties of voids in cDE and ΛCDM. Left panel: ratio of radii for voids in cDE matched to voids in ΛCDM as a function of ΛCDM void size. If the void has no match, it is given a relative radius of 0. Right panel: Relative distance versus relative radius for matched voids. The gray lines marking unity in each panel are to guide the eye. Walls between smaller and mid-scale voids are thinned out in the cDE model, making them appear as single, larger voids.

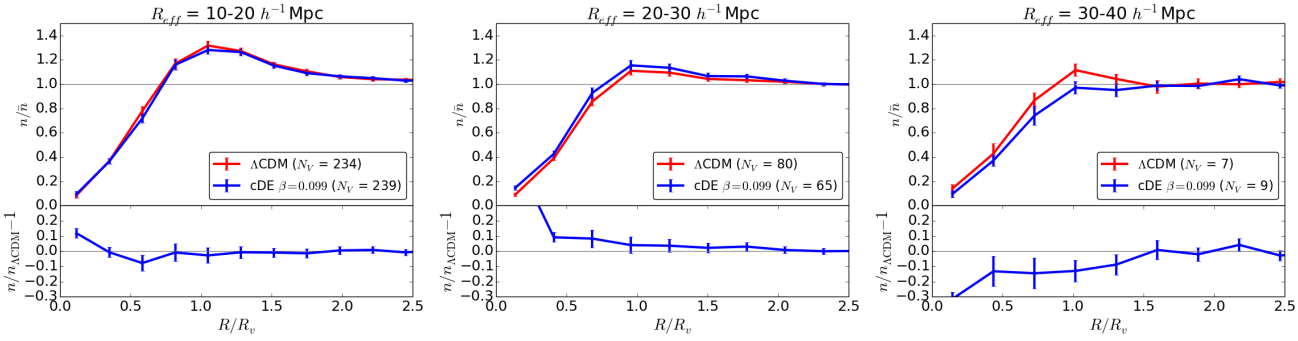
R_{eff} = 10-20 h^{-1} Mpc
R_{eff} = 20-30 h^{-1} Mpc
R_{eff} = 30-40 h^{-1} Mpc
ΛCDM (N_V = 234)
cDE β=0.099 (N_V = 239)
ΛCDM (N_V = 80)
cDE β=0.099 (N_V = 65)
ΛCDM (N_V = 7)
cDE β=0.099 (N_V = 9)
$n/\bar{n}$
$n/n_{\Lambda CDM} - 1$
R/R_v

Figure 3. One-dimensional radial density profiles of stacked voids with 1σ bootstrapped uncertainties (points with error bars). The bottom of each panel shows the cDE profile relative to the ΛCDM one. The solid lines are to guide the eye. Shown are profiles from the ΛCDM (red) and cDE (blue) simulations. The legend indicates the number of voids N_v in each stack. Coupling enhances the compensation walls of medium-scale voids but diminishes the walls of larger voids.

$\delta_c \sim -0.8$, regardless of size. However, the evolution of the scaling radius as a function of void size is significantly different between the two models. Indeed, the largest cDE voids in this volume become undercompensated, whereas no ΛCDM voids reach the necessary scales. Since almost all ΛCDM voids can be matched to a cDE counterpart, Figure 2 also allows us to interpret these results: the larger cDE voids are actually merged — not enlarged — ΛCDM voids, making the voids appear uniformly larger without greatly affecting the central densities. As in the profiles themselves, the differences between individual profiles are only statistically significant for the largest radius bin. However, there are relatively few voids here, and we may be underestimating the true uncertainty.

We also examined ellipticities using the inertia tensor method as described in Bos et al. (2012) and Sutter et al. (2013). However, as Bos et al. (2012) discovered, in sparse populations such as galaxies it is very difficult to statistically separate ΛCDM from alternative cosmologies using void shapes. We found no significant distinctions in the ellipticities.

4 CONCLUSIONS

We have examined the effects on voids due to coupling between dark matter and dark energy with realistic galaxy survey volumes and tracer densities and provided an initial assessment of the feasibility of current surveys to detect the coupling with voids. We have found that the coupling produces much larger voids compared to ΛCDM mostly by merging medium-scale voids. Additionally, we have quantified the effects of coupling on the radial density profiles by finding the best fits to the analytic HSW profile, and found that DM-DE coupling can more easily make voids underdense.

Traditional probes of large-scale structure such as the power spectrum have difficulty differentiating cDE models from ΛCDM (e.g., Carlesi et al. 2014), but voids are exceptionally powerful discriminating tools. We have studied

a relatively weak coupling strength; thus even a null result would be informative about the capabilities of void properties to distinguish these models. However, even with limited survey volumes and only ~ 400 total voids the number functions are distinguishable in a statistically significant manner. Density profiles of the largest voids, despite the relatively few number of voids, also provide measurable differences in the scaling radius r_s of the HSW profile, although future simulations with larger volumes will be needed to verify the precise statistical significance of these profile differences.

The void population we have studied is fairly representative of — and accessible with — current low-redshift galaxy surveys (Sutter et al. 2012b). These results may explain the large void identified by Tavasoli et al. (2013). In addition, using Halo Occupation Distribution modeling (Berlind & Weinberg 2002) and accounting for survey geometries, Sutter et al. (2013) was able to match ΛCDM simulations to observed void populations. Thus, coupled DM-DE may already be measurable with current data sets. However, for a complete comparison of the void abundance we must include mask effects (Sutter et al. 2013). We also have not included the effects of galaxy bias and distortions to the density profiles from peculiar velocities. However, we can use techniques such as those presented by Pisani et al. (2013) to construct the real-space profile without modeling. We will save a more detailed comparison and measurement of a constraint for future work.

This study is only an initial assessment comparing one cDE model to ΛCDM, using simulations optimized to study the properties of high-density clusters. We also examined other coupling strengths (Eq. 4) but did not find significant differences among the models with this limited void population. We are preparing larger simulations that will allow us to examine the detailed relationship between coupling strength and void properties and assess the ability of high-redshift galaxy surveys such as BOSS (Dawson et al. 2013) to probe these cosmologies using voids. In addition, future galaxy surveys will only serve to increase the statistical significance of these differences, leading to ever-further constraints on these models.

ACKNOWLEDGMENTS

PMS and EC thank Alexander Kusenko and the NSF for the PACIFIC2013 workshop, where this work was initiated. The authors thank the referee for the highly constructive comments that substantially improved this letter, as well as Nico Hamaus, Alice Pisani, and Ravi Sheth. BDW acknowledges funding from an ANR Chaire d'Excellence (ANR-10-CEXC-004-01), the UPMC Chaire Internationale in Theoretical Cosmology, and NSF grants AST-0908 902 and AST-0708849. This work made in the ILP LABEX (under reference ANR-10-LABX-63) was supported by French state funds managed by the ANR within the Investissements d'Avenir programme under reference ANR-11-IDEX-0004-02.

AK is supported by the *Ministerio de Economía y Competitividad* (MINECO) in Spain through grant AYA2012-31101 as well as the Consolider-Ingenio 2010 Programme of the *Spanish Ministerio de Ciencia e Innovación* (MICINN) under grant MultiDark CSD2009-00064. He also acknowledges support from the *Australian Research Council* (ARC) grants DP130100117 and DP140100198. He further thanks Ghosts I've Met for winter's ruin.

REFERENCES

Abazajian K. N., et al., 2009, Astrophys. J. Supp., 182, 543
Ahn C. P., et al., 2012, Astrophys. J. Supp., 203, 21
Baldi M., Pettorino V., Robbers G., Springel V., 2010, Mon. Not. R. Astron. Soc., 403, 1684
Berlind A. A., Weinberg D. H., 2002, ApJ, 575, 587
Biswas R., Alizadeh E., Wandelt B., 2010, Phys. Rev. D, 82
Bos E. G. P., van de Weygaert R., Dolag K., Pettorino V., 2012, ArXiv e-prints: 1205.4238
Carlesi E., Knebe A., Lewis G. F., Wales S., Yepes G., 2014, Mon. Not. R. Astron. Soc., 439, 2943
Carlesi E., Knebe A., Lewis G. F., Yepes G., 2014, Mon. Not. R. Astron. Soc., 439, 2958
Chiba T., De Felice A., Tsujikawa S., 2013, Phys. Rev. D, 87, 083505
Clampitt J., Cai Y.-C., Li B., 2013, Mon. Not. R. Astron. Soc., 431, 749
Dawson K. S., et al., 2013, AJ, 145, 10
Hamaus N., Sutter P. M., Wandelt B. D., 2014, ArXiv e-prints: 1403.5499
Jennings E., Li Y., Hu W., 2013, Mon. Not. R. Astron. Soc., 434, 2167
Kreckel K., Ryan Joung M., Cen R., 2011, ApJ, 735, 132
Lavaux G., Wandelt B. D., 2010, Mon. Not. R. Astron. Soc., 403, 1392
Li B., 2011, Mon. Not. R. Astron. Soc., 441, 2615
Li B., Zhao G.-B., Koyama K., 2012, Mon. Not. R. Astron. Soc., 421, 3481
Li B., Zhao H., 2009, Phys. Rev. D, 80
Muller V., Arbabi-Bidgoli S., Einasto J., Tucker D., 2000, Mon. Not. R. Astron. Soc., 318, 280
Neyrinck M. C., 2008, Mon. Not. R. Astron. Soc., 386, 2101
Nusser A., Gubser S. S., Peebles P., 2005, Phys.Rev., D71, 083505
Pan D. C., Vogeley M. S., Hoyle F., Choi Y.-Y., Park C., 2012, Mon. Not. R. Astron. Soc., 421, 926
Peebles P. J. E., 2001, ApJ, 557, 495
Peebles P. J. E., Ratra B., 1988, ApJ, 325, L17
Pisani A., Lavaux G., Sutter P. M., Wandelt B. D., 2013, ArXiv e-prints: 1306.3052
Planck Collaboration 2013, ArXiv e-prints: 1303.5076
Ratra B., Peebles P. J. E., 1988, Phys. Rev. D, 37, 3406
Reid B. A., et al., 2012, Mon. Not. R. Astron. Soc., 426, 2719
Spolyar D., Sahlén M., Silk J., 2013, ArXiv e-prints: 1304.5239
Springel V., 2005, Mon. Not. R. Astron. Soc., 364, 1105
Sutter P. M., et al., 2014, ArXiv e-prints: 1406.1191
Sutter P. M., Lavaux G., Wandelt B. D., Weinberg D. H., 2012a, ApJ, 761, 187
Sutter P. M., Lavaux G., Wandelt B. D., Weinberg D. H., 2012b, ApJ, 761, 44
Sutter P. M., Lavaux G., Wandelt B. D., Weinberg D. H., Warren M. S., 2013, ArXiv e-prints: 1310.7155
Sutter P. M., Lavaux G., Wandelt B. D., Weinberg D. H., Warren M. S., 2014, Mon. Not. R. Astron. Soc., 438, 3177
Sutter P. M., Lavaux G., Wandelt B. D. Hamaus N., Weinberg D. H., Warren M. S., 2013, ArXiv e-prints: 1309.5087
Sutter P. M., Ricker P. M., 2008, ApJ, 687, 7
Tavasoli S., Vasei K., Mohayaee R., 2013, Astron. & Astrophys., 553, A15
Tinker J. L., Conroy C., 2009, ApJ, 691, 633
Wang P.-Y., Chen C.-W., Chen P., 2012, Journal of Cosmology and Astroparticle Physics, 2, 16